Fault Diagnosis of Synchronous Generator Based on Adaptive Chirp Mode Decomposition Permutation Entropy and Deep Learning

Chao Zhang, RuiQing Jin and ChenXin Li
Department of Mechanical Engineering and the Hebei Key Laboratory of Electric Machinery Health Maintenance and Failure Prevention, North China Electric Power University, Baoding, 07100, China.
E-mail: 153076594@qq.com

(Received 15 May 2023; accepted 3 September 2023)

Generators are subject to extreme environmental conditions that can cause critical areas to gradually break down, potentially leading to catastrophic failures. This paper proposes a hybrid method for generator fault diagnosis. Firstly, adaptive chirp mode decomposition (ACMD) is applied to decompose the vibration signal into five intrinsic mode function (IMF) components. Then, the permutation entropy (PE) of each IMF is calculated to construct the feature vector. The deep learning part of the proposed method uses convolutional neural network (CNN) as a classifier to recognize different faults. Finally, the visualization result using t-Distributed Stochastic Neighbor Embedding (t-SNE) is presented. The result of classification suggests that the method proposed in this paper realizes fault diagnosis with the accuracy of 98%, which has a higher recognition rate than other methods mentioned in this paper.

1. INTRODUCTION

The generator is the most critical component in the electrical system and is susceptible to various faults due to its complex and variable working environment. Common issues include stator inter-turn short circuits, eccentricity, or other mechanical faults, which can damage the generator and even result in a critical accident[1]. To prevent significant human and economic losses caused by generator faults, it is significant to explore methods for generator fault diagnosis in early stage.

To effectively monitor the operating status of the generator, various sensor systems have gathered many variables related to the generator operating characteristics, including temperature, current, voltage, vibration, etc. If the fault information hidden in these data can be extracted, the operational status of generator can be confirmed, and faults can be diagnosed as early as possible. Many researchers spare no effort to explore simple and effective methods in the field of generator fault diagnosis. Their focus has primarily been on voltage, current, and other electrical parameters, as well as vibration signal. In aspect of electrical parameters, T. Goktas et al. realized the diagnosis of static eccentricity faults and the discernment of broken magnet based on stator phase current waveform and electromotive force.[2] I. O. Zaparoli et al. diagnosed inter-turn short circuit fault through transient envelope current analysis in the induction motor stator.[3] Meanwhile, Ma et al. used the phase-angle of the branch current as diagnostic indicators for the diagnosis of synchronous condensers, but they ignored generality and difficulty in obtaining phase current in real conditions.[4] While electrical parameters are an excellent choice for diagnosing electrical equipment, the abundant fault information hidden in the vibration signal should not be underestimated. Most vibration signal-based methods are mainly applicable to rotating machinery such as bearings and gears.[5,6] Since the generator also falls under the category of rotating machines, and it is necessary to introduce the fault diagnosis methods for rotating machinery into generator fault diagnosis to obtain the characteristic of fault and realize the fault classification based on vibration signal.

Many scholars are constantly exploring advanced signal processing technology and the signal processing technology has made considerable advance over the past decades.[7] For instance, Huang et al. proposed the empirical mode decomposition (EMD) method in 1998, which can decompose a signal into a combination of several intrinsic mode functions (IMFs).[8] However, this method is plagued by the problem of endpoint effect and mode mixing. Then, to address the problem shown in EMD, Wu et al. developed ensemble empirical mode decomposition (EEMD) based on EMD with a better decomposition effect by adding white Gaussian noise.[9] This method has been generally applied in fault pattern recognition.[10,11] Although adding white noise to the original signal can solve the problem of mode mixing, there is a problem where the average white noise cannot be offset, resulting in the inability to ignore noise in the reconstructed signal. Thus, Torres M. E. et al. proposed complete ensemble empirical mode decomposition with adaptive noise (CEEMDAN) by adding IMF components of white noise, which effectively reduces the residual noise in the reconstructed signal and decreases the reconstruction error.[12] Konstantin D. et al. proposed variational mode decomposition (VMD) to decompose the signal into several IMF components by solving a variational problem. VMD algorithm can arbitrarily choose the number of components while overcoming the problem of mode mixing and endpoint effect. But the penalty coefficient and mode number need to be manually set in advance.[13] Since then, with the purpose of obtaining a better decomposition effect, various signal decomposition algorithms have emerged. Empirical wavelet transform (EWT) is a method that can localize signals in both the time and frequency domains for analysis with strong adaptability and denoising ability, but the decomposition process is extremely time-consuming due to high computational complexity.[14] Adaptive local iterative filtering (ALIF) proposed by Antonio C. et al. faces the same problem as EWT, which has a high computational accuracy but a complicated calculation process.[15] These methods have been applied to obtain the fault feature information hidden in the vibration signal collected from the generator. Although these methods have already achieved satisfactory results, there still have shortcomings that need to be overcome. Firstly, the signal decomposition process is extremely complicated and time consuming because the vibration signal required to decompose into numerous components and a quantity of useless sub-band components will be created. Then, the parameters of these methods need to be preset before decomposition, making it difficult to ensure the optimal selection of each parameter.[16] Recently, a novel signal decomposition method named adaptive chirp mode decomposition (ACMD) is proposed.[17] Compared to these methods mentioned above, this method can extract specific modes with abundant feature information directly without unnecessary components, and it requires fewer preset parameters. Consequently, this method is applied to generator fault diagnosis in this paper.

To characterize the features contained in the signal processed by processing algorithms, complexity theory has been extensively applied to evaluate the complexity of signals and extract fault feature information hidden in signals. Permutation entropy, as an effective complexity evaluation method, has achieved excellent results in the field of fault diagnosis. Zhang et al. input the feature vector composed of permutation entropy values into the subsequent classifier, which achieved satisfactory clustering results.[18] The experimental results showed the superiority of permutation entropy compared to other complexity evaluation methods, such as approximate entropy (AE), sample entropy (SE), dispersion entropy (DE) etc. Thus, the permutation entropy is applied as the feature vector to evaluate the complexity of signals decomposed by signal processing algorithms in this paper.

Although signal processing algorithms can realize fault diagnosis with excellent results, operators require extensive basic knowledge of signal processing and practical experience to complete the task. In an actual working environment, it can be difficult to achieve the fault diagnosis without expert guidance. Machine learning algorithms provide a solution to this dilemma by directly classifying massive amounts of fault information, omitting the need for human involvement. To solve the problems in practical engineering conditions, various classification algorithms have been applied in the actual engineering environment such as the artificial neural network (ANN), the support vector machine (SVM) etc.[19,20] By combining the strong decomposition ability of signal processing technique with the powerful classification capacity of machine learning algorithms, a concise and effective method has appeared to realize fault diagnosis. Zhang et al. proposed an ANN model with modified EEMD for fault diagnosis of asynchronous motor.[21] Tang et al. realized the fault diagnosis of hydraulic generator bearing and achieved high classification accuracy through the model of VMD-SVM.[22] These machine learning classification algorithms still have their own disadvantages to overcome. While the artificial neural network is capable of fault classification when processing a large amount of data, adjusting the network structure parameters can be time-consuming. The SVM has been extensively applied in fault diagnosis, however, when it comes to a large amount of data, the processing capacity is limited, and the training speed will significantly decrease.

The emergence of deep learning algorithms provides a solution for these problems, such as long short-term memory (LSTM), CNN and so on, which had been generally applied for fault detection and diagnosis for different objects. Masoud Jalayer et al. developed a convolutional LSTM and continuous wavelet transforms model to complete the fault detection and diagnosis for rotating machinery.[23] Deng et al. applied VMD and CNN model to achieve incipient cable fault recognition and classification.[24] He et al. simultaneously optimized the VMD and CNN and applied them to realize the fault diagnosis of flywheel bearing, achieving extremely high classification accuracy.[25] Even CNN and LSTM are commonly used in tandem for wind turbine bearings fault diagnosis due to their unique advantage.[26] These deep learning algorithms ensure both diagnostic accuracy and diagnostic efficiency. Thus, to realize the fault diagnosis as early as possible, ACMD, PE and CNN are applied to realize fault feature extraction and classification of the generator. The following are the primary contributions of this study:

1. A signal processing algorithm named ACMD is utilized to generator diagnosis based on vibration signal instead of electric parameter.
2. The PE is applied to extract fault feature information hidden in vibration signals.
3. Combining with the advantages of signal processing technology and machine learning, a hybrid model of the ACMD PE and CNN is proposed.
4. The effectiveness and superiority are proved by comparing with other methods.

The subsequent sections of this paper are organized as follows: Section 2 presents an overview of the fault classification methodologies proposed in this paper, which include ACMD, permutation entropy, and CNN. In section 3, the complete fault diagnosis process of synchronous generator based on ACMD, PE and CNN is discussed. Section 4 presents the results of the proposed method, including model diagnosis and visualization analysis, and the effectiveness and superiority of the method are demonstrated through comparative analysis. Finally, section 5 of this paper provides a summary of the conclusions drawn from the proposed method and outlines the prospects for future research work.

2. THEORY

2.1. Adaptive Chirp Mode Decomposition

The core idea of adaptive chirp mode decomposition (ACMD) is to use a greedy algorithm to decompose the signal into multiple components. The decomposition process can be described as follows:[17] For one signal component, the problem defined in Eq. (1) needs to be solved

$$\min_{m_i(t),n_i(t),f_i(t)} \left\{||\ddot{m}_i||_2^2 + ||\ddot{n}_i + \alpha||s(t) - s_i(t)||_2^2\right\};$$
$$s.t. \begin{cases} s(t) & = \sum_{i=1}^{K} s_i(t) \\ s_i(t) & = m_i(t)\cos\left[2\pi\int_0^t f_p(\tau)d(\tau)\right]; \\ & +n_i(t)\sin\left[2\pi\int_0^t f_p(\tau)d(\tau)\right] \end{cases} \tag{1}$$

where $s(t)$ is the original signal, $s_i(t)$ is called the i-th chirp mode of $s(t)$, $||s(t) - s_i(t)||_2^2$ represents the remaining energy after the estimated component is removed, $\alpha > 0$ is a weighting coefficient, $f_i(\tau)$ is the instantaneous frequency of the i-th chirp mode, $m_i(t)$ and $n_i(t)$ represent the corresponding demodulated signals of $s_i(t)$.

For a series of the digital signal with N samples, Eq. (1) can be expressed in a discrete form as follows:

$$\min_{u_i(t), f_i(t)} \{||\Theta u_i||_2^2 + \alpha||s - G_i u_i||_2^2\}; \tag{2}$$

where $\Theta = \begin{bmatrix} \Omega & \\ & \Omega \end{bmatrix}$, Ω is a second-order difference matrix, $u_i = [m_i^T, n_i^T]$ with $m_i^T = [m_i(t_0), \ldots, m_i(t_{N-1})]^T$, $m_i^T = [n_i(t_0), \ldots, n_i(n_{N-1})]^T$ and $m_i^T = [s_i(t_0), \ldots, s_i(s_{N-1})]^T$.

$$G_i = [C_i, S_i]; \tag{3}$$

$$C_i = \text{diag}[\cos(\phi_i(t_0)), \ldots, \cos(\phi_i(t_{N-1}))]; \tag{4}$$

$$S_i = \text{diag}[\sin(\phi_i(t_0)), \ldots, \sin(\phi_i(t_{N-1}))] \tag{5}$$

where $\phi_i(t) = 2\pi \int_0^t f_i(\tau) d\tau$.

By solving a l2-regularized least-squares problem, vector u_i, which is created by the demodulated signals, can be estimated when given a frequency function $f_i(t)$ (or matrix G_i), as shown in Eq. (2). Therefore, an iterative algorithm can be employed to solve the above problem by alternately updating the vector ui. In the j-th iteration, the vector ui is updated as follows: where G_i^j is a matrix consisted of the instantaneous frequency, j refers to the number of iterations. Then the mode can be estimated as

$$s_i^j = G_i^j u_i^j; \tag{6}$$

The variation ξ between two adjacent iterations of the modes can be computed as follows:

$$\xi_i^j = ||s_i^j - s_i^{j-1}||_2^2 / ||s_i^j||_2^2. \tag{7}$$

The iterative decomposition steps described above continue until the difference value between the modes in two adjacent iterations is within the predetermined stopping criterion. Following the iterative decomposition process described above, once the stopping criterion is met, the estimated mode can be obtained.

2.2. Permutation Enthropy

Permutation entropy is a technique used for quantifying the complexity of non-stationary and chaotic time series signals, particularly in the presence of intricate and varying noise[28] Permutation entropy is particularly well-suited for fault diagnosis in rotating machinery due to its excellent superiority in reflecting the tiny abrupt change of vibration response in the whole mechanical system. The algorithm operates based on the following principle: Given a set of time series $\{x_i | i = 1, 2, \ldots, N\}$; then, reconstruct the phase space.

$$X_I = [x_i, x_i + \tau, \ldots, x_i + (m-1)\tau]; \tag{8}$$

where the τ is delay time and the m is the embedding dimension.

The number of permutations of any X_i in time series is $m!$, the probability of any permutation occurring in $m!$ permutations is:

$$P(\omega) = \frac{T(\omega)}{N - (m-1)\tau} \tag{9}$$

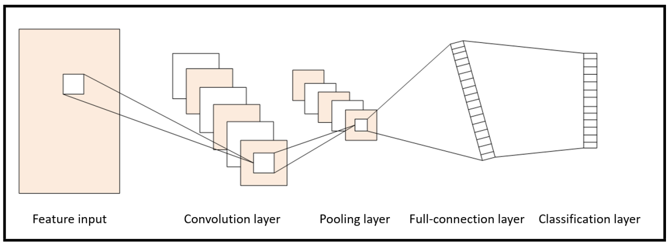

Figure 1. The basic structure of CNN.

where the ω is any permutation occurring in $m!$ permutations, $T(\omega)$ indicates that the number of times ω appears.

Then the PE can be described as:

$$H_{PE} = -\Sigma P(\omega) \ln P(\omega); \tag{10}$$

After the normalization,

$$PE = \frac{H_{PE}}{\ln(m!)}. \tag{11}$$

The PE algorithm evaluates the complexity and variability of time series signals. A higher value of PE indicates a greater complexity of the signal, while a lower value indicates the opposite. The selection of parameters also has a significant impact on the calculation result of PE. The constructed feature vector contains little information if m is too small, making the application of this algorithm meaningless. If the value of m is too large, the time series would homogenize by a reconstructed phase space, which would spend a lot of time on calculating values. By comparison, the selection of delay time τ has little effect on the algorithm.[27]

2.3. Convolutional Neural Network

The convolutional neural network is a widely used deep learning algorithm that possesses remarkable learning capability and adaptability owing to its intricate network architecture, making it capable of processing complex multidimensional data. The typical structure of a convolutional neural network consists of an input layer, convolutional layer, pooling layer, fully connected layer, and classifier layer, as shown in Fig. 1.[28]

In the convolutional layer, the input characteristic matrix is calculated by fixed-sized convolutional kernel and activated by activation function. The calculation process of convolutional layer is as follows:

$$a_n^l = f\big(\sum_{\forall m} a_m{}^{l-1} * k_{m,n}^l + b_n^l\big); \tag{12}$$

where the a_n^l is the n-th feature map in l-th layer, $k_{m,n}^l$ is convolutional kernel between two characteristic maps, b_n^l is bias and f is nonlinear activation function.

In the pooling layer, the output feature from convolutional layer is merged and reduced in dimension to prevent the overfitting of the network model. According to the different downsampling methods, the pooling layer is divided into two ways, namely maximum pooling, and average pooling. As shown in Fig. 2, the pooling kernel scale is 2×2, and the step size is 2. The 4×4 image or feature map is divided into four different regions, and the maximum or mean values are taken from each of the four different regions to represent the information of each region.

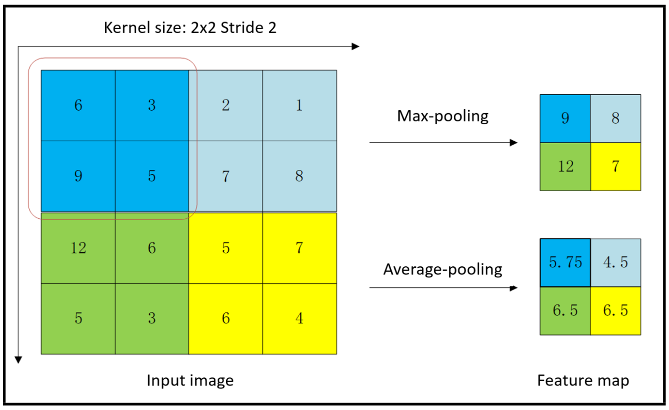

Figure 2. Schematic diagram of pooling in different ways.

For max pooling (MP) or average pooling (AP), the expression is as follows:

$$MP(R_k) = \max_{i \in R-k} c_i; \tag{13}$$

$$AP(R_k) = \frac{1}{|R_k|} \sum_{i \in R_k} c_i; \tag{14}$$

where the R_k represents the k-th local statistical information of the feature map, and c_i is the i-th activation value of the local statistical information.

Maximum pooling is selected as pooling method in this paper. The selection of size of pooling layer must be appropriate, otherwise the critical information would be omitted if the size is too small or large.

In the full-connection layer, the full-connection form is mainly used to realize the one-dimensional expansion of the output features from the previous layer, to facilitate the classification and recognition of the next layer.

At the classification level, according to the one-dimensional feature vector expanded at the full connection, the model is trained and classified with the help of the relevant classification recognizer. At present, the Logistic and the Soft-max are generally applied as classification methods in the classifier layer, and Soft-max method is utilized in this study.

3. PROCESS OF THE PROPOSED MODEL

In this section, a detailed description of the proposed fault diagnosis model based on ACMD, PE, and CNN is presented, as shown in Fig. 3. The steps involved in the diagnosis modeling process are as follows:

- Step 1: Conduct ACMD algorithm to obtain K IMF components;
- Step 2: Calculate the permutation entropy of each IMF using formula (12) and construct the feature vector matrix composed of K permutation entropy values;
- Step 3: Divide the feature vectors obtained in step 2 proportionally into training and test sets.
- Step 4: Use CNN to classify the different kinds of generator fault and output the diagnostic result.

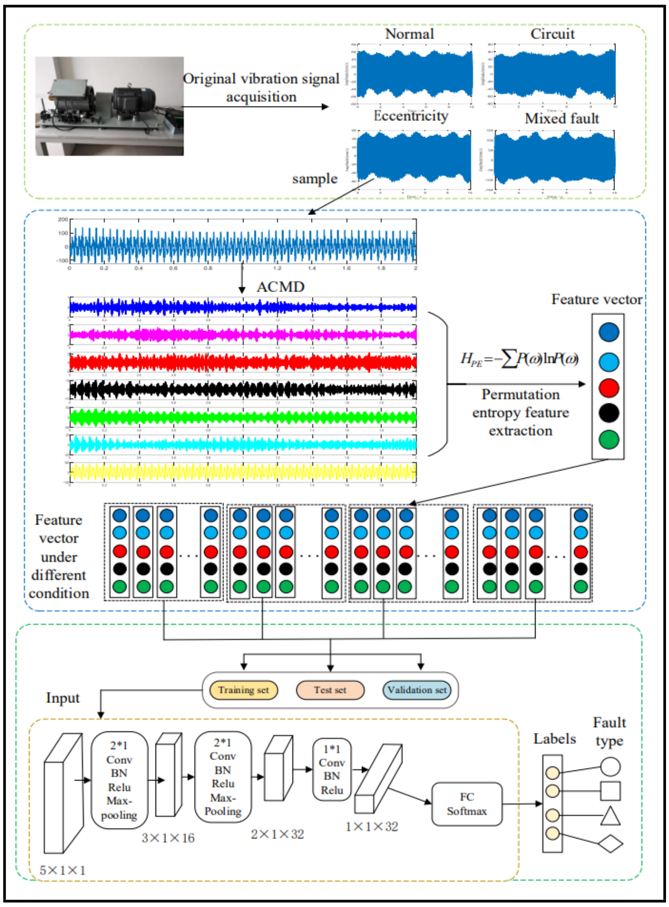

Figure 3. The process of fault diagnosis.

Table 1. The structural parameters of CS-5 fault simulation motor.

Parameter	Value	Parameter	Value
Rated power	5 kW	Pole pairs	1
Rated stator current	9.0 A	Rated stator voltage	321 V
Rated speed	1500 r/min	Radial air gap length	1.2 mm

4. EXPERIMENTAL VERIFICATION

4.1. Data Acquisition

The vibration signals related to generator faults used in this study are obtained from the CS-5 fault simulation generator. The appearance of CS-5 fault simulation generator is presented in Fig. 5. The sampling frequency f_s is set at 5000 Hz while the number of sample point is 10000. Other main parameters of the generator are shown in Tab. 1. Normal condition and three classical fault types of generators were selected in this study, including stator eccentricity, stator inter-turn short circuit, short circuit, and eccentric mixed fault. The total number of experimental data is 480 groups, and each fault type includes 120 samples. The vibration signals of generator under four different fault conditions are shown in Fig. 4, and the basic structure of convolutional neural network is shown in Fig. 6.

4.2. Diagnose Preparation

4.2.1. The Order of IMF

The selection of the order of IMF had a significant impact on the accuracy of fault classification. If the order was too small, the feature vector may not have contained enough fault information, leading to low classification accuracy. Conversely, if the order was too large, the calculation process became overly

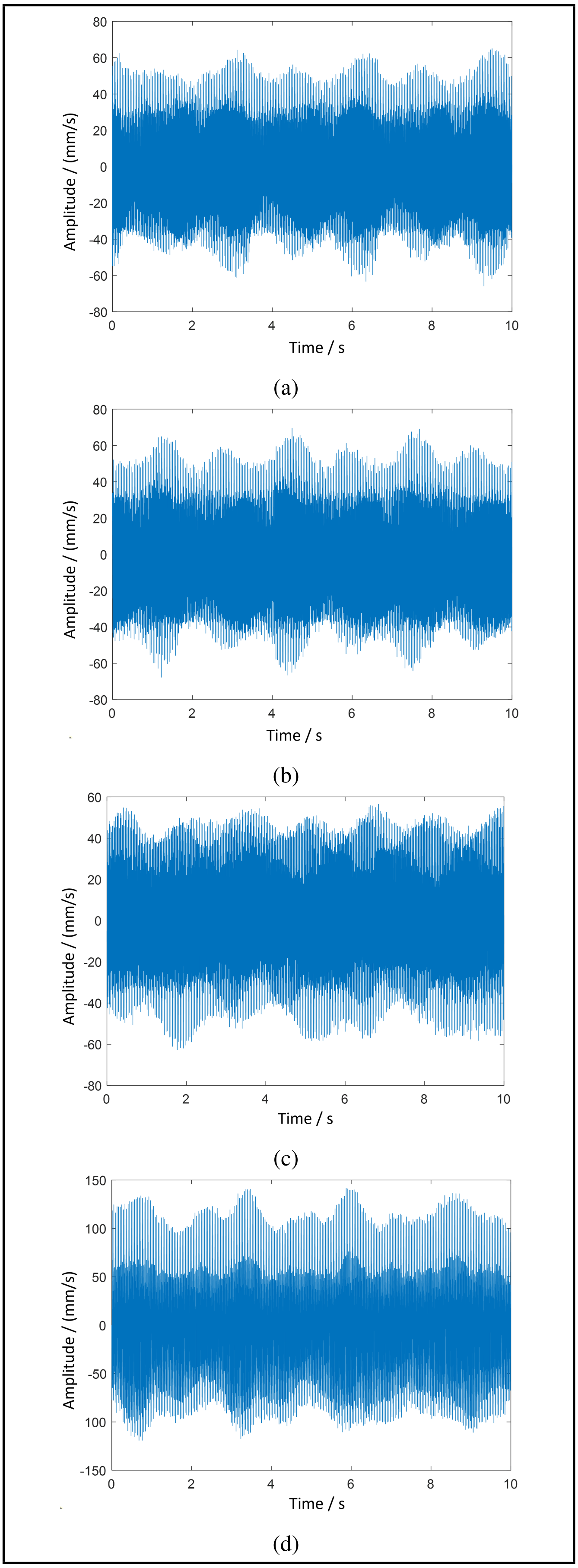

Figure 4. Time domain signal of generator under four different states: (a) Normal; (b) Inter-turn short circuit fault; (c) Eccentricity fault; (d) Short circuit and eccentricity mixed fault.

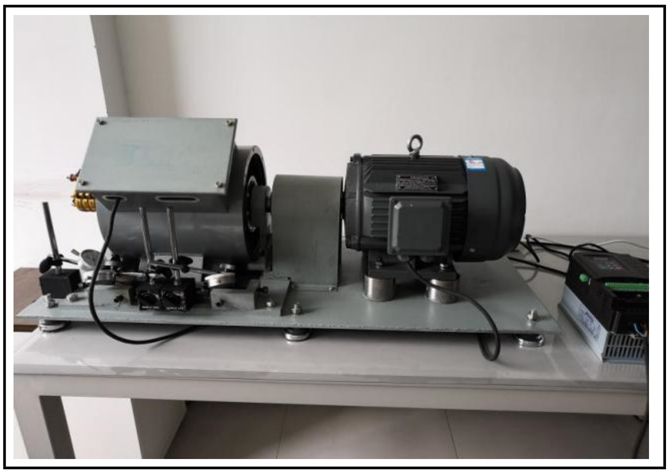

Figure 5. The appearance of CS-5 fault simulation generator.

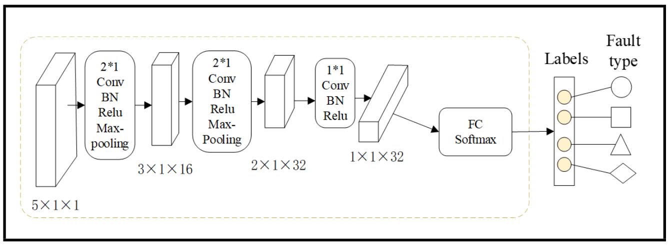

Figure 6. The structure of convolutional neural network.

Table 2. Correlation coefficients of different order components of signal.

Order	Value	Order	Value
1	0.8989	6	0.0339
2	0.3467	7	0.0316
3	0.3554	8	0.0253
4	0.3486	9	0.0180
5	0.1606	10	0.0155

complicated, resulting in unnecessary time wastage. Therefore, it was important to choose an appropriate IMF order.

One way to access the similarity between two signals was calculating the correlation coefficient between the original signal and the target signal. The result closer to 1 indicates a higher similarity, whereas a result closer to 0 indicates the opposite. In this study, we applied the correlation coefficient method to determine the order of IMF. At first, the signal of stator inter-turn short circuit and stator eccentricity mixed fault, which obtains the most fault information, was selected as the example to be decomposed. Then, the signal was decomposed into 10-order IMF components through ACMD algorithm. Subsequently, the correlation coefficients between each order component and the original signal are calculated. The results of the calculations are shown in Tab. 2. As shown, the value of correlation coefficient continuously decreases and is not reduced to below 0.1 until the number of orders increases to 6. The smaller value indicates the weaker correlation between the IMF component and original fault signal. Finally, based on the result in the Tab. 2, the reasonable number of IMF component is set at 5.

4.2.2. Parameter of ACMD

The only parameter of ACMD algorithm needs to be preset is the weighting coefficient α, which would affect the bandwidth of estimated mode. The value of α is usually set between 0.01 and 0.0001. To find the most appropriate value, the

Table 3. Parameters of the simulating signal.

Amplitude	Value	Frequency	Value	Phase	Value
A_0	8	f_0	50	φ_0	$2\pi/3$
A_2	10	f_2	150	φ_2	$\pi/6$
A_3	5	f_3	200	φ_3	$\pi/3$
A_4	4	f_4	250	φ_4	$\pi/4$
A_5	5	f_5	300	φ_5	$\pi/3$
A_6	3	f_6	350	φ_6	$\pi/6$
A_7	5	f_7	400	φ_7	$2\pi/3$
A_8	3	f_8	450	φ_8	$\pi/6$
A_9	7	f_9	500	φ_9	$\pi/3$

envelope spectrum of stator inter-turn short circuit and eccentricity mixed fault is shown in Fig. 6 under different α from 0.01 to 0.0001. According to the research in Ref.,[1] the amplitude of $1 \sim 10f$ ($f = 50$ Hz was the fundamental frequency of the generator) will increase evidently and can be seen in the frequency spectrum. It can be seen from Fig. 7 (a) that the $1 \sim 10f$ of the generator can be vividly found in the envelope spectrum when the α is set at 0.01. However, only the $1\ 6f$ can be found in Fig. 7 (b) when the α is set at 0.001, and the $1-4f$ can be found when the α is set at 0.0001, which is completely inconsistent with previous research results. Compared Fig. 7 (a) with Fig. 7 (b) and Fig. 7(c), the main difference is reflected in the existence of $7-10f$, which illustrates that the vibration signal contains abundant and accurate fault information. Thus, 0.01 is selected as the most appropriate parameter.

4.2.3. Application Of ACMD On Simulation And Real Signal

It is essential to make further efforts to prove the effectiveness and superiority of ACMD after determining the parameters of ACMD. Thus, the result of signal processing was compared with VMD algorithm. Before adapting to the real fault vibration signal, a simulation signal under the hybrid fault state of stator eccentricity and short circuit was studied. According to the conclusion in Ref.,[1] the amplitude $1-10f$ will increase significantly and the enormous noise will appear simultaneous when the fault occurs19 in the generator. To accurately simulate the fault vibration signal, a simulation signal is designed as:

$$\begin{aligned} x(t) = A + A_0 \cos(2\pi f_0 t + \varphi_0) + \\ A_1 \cos(2\pi f_1 t + \varphi_1) + \\ \cdots + A_8 \cos(2\pi f_8 t + \varphi_8) + \\ A_9 \cos(2\pi f_9 t + \varphi_9) + n(t;) \end{aligned} \tag{15}$$

where A is the direct-current component contained in $x(t)$; $A_i \cos(2\pi f_i t + \varphi_i)$ refer to the ten main components of the vibration signal to simulate the characteristic frequencies of the stator eccentricity and short circuit fault; $n(t)$ is a Gaussian white noise and signal-to-noise ratio is 30 dB. The value of A is arbitrary, and the detailed parameters of the simulating signal are shown in Tab. 3.

To verify the credibility of the experiment, reconstructed signal, which was composed of first five IMF, it was determined as the optimum mode component to apply in both ACMD and VMD algorithms. The envelop diagrams of the simulation signal are drawn, respectively, as shown in Fig. 8 (a) and Fig. 8 (b). The envelop spectrum of the simulation signal processed by ACMD not only has evident characteristic frequency, but also is not influenced by Gaussian white noise.

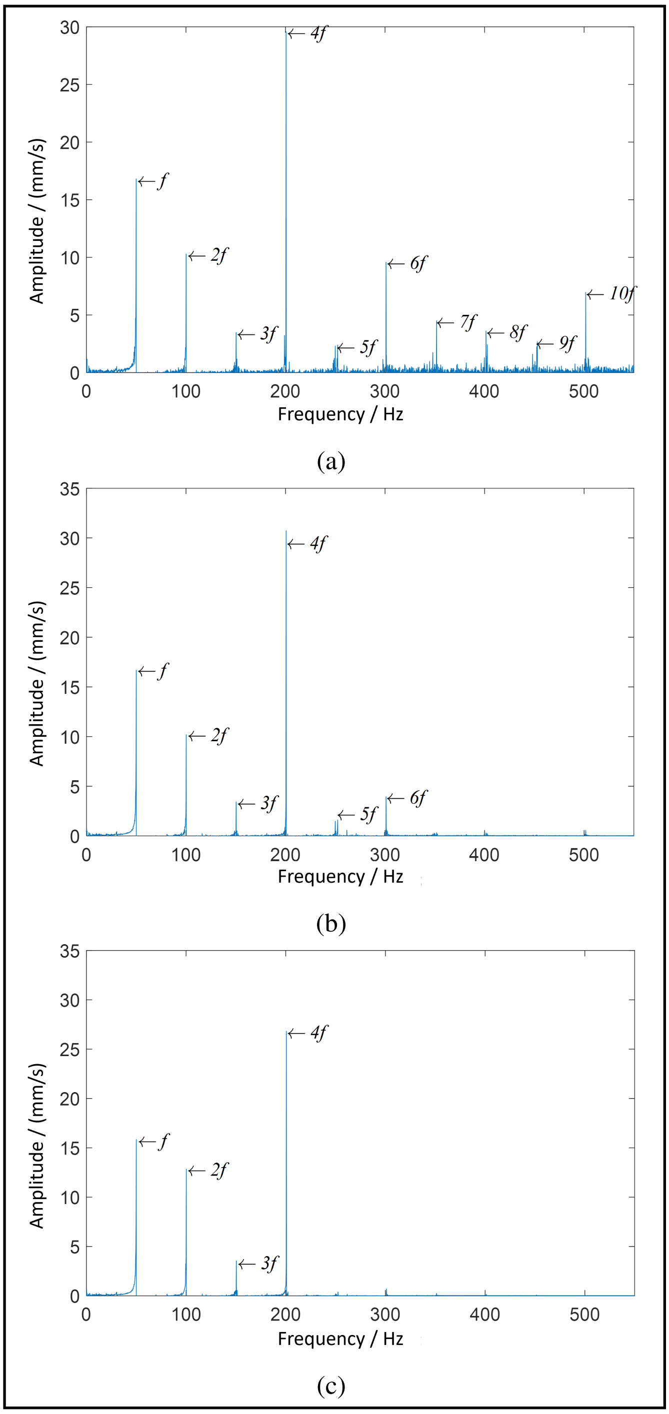

Figure 7. ACMD envelope spectrum under different α: (a) $\alpha = 0.01$; (b) $\alpha = 0.001$; (c) $\alpha = 0.0001$.

As a comparison, the $1-3f$ and $8-10f$ can be found in Fig. 8 (a). The $4-6f$ components are submerged in Gaussian white noise.

Regarding the real generator fault, the stator eccentricity and short circuit mixed fault was chosen, and the results of the envelope spectrum analysis of VMD and ACMD are carried out in Fig. 8. As can be seen from Fig. 8 (c), the peak of $1-2f$, $4-6f$ and $8-10f$ frequency components are apparent, $3f$ and $7f$ frequency components disappear in the envelope spectrum. On the contrary, as shown in Fig. 8 (d), there are several manifest peak spectrum lines at each fault characteristic frequency which indicates that stator inter-turn short circuit and stator eccentricity mixed fault occurs in the generator. In addition, the envelope spectrum lines are not interfered from redundant frequency. The analysis result of the simulation fault signal is consistent with the actual situation and the superiority of ACMD is proved by comparing with VMD.

4.3. Generator Diagnosis Analysis

This section presents the detailed processing results of the proposed method to demonstrate its effectiveness. According to many studies on deep learning algorithms for fault diagnosis, the number and proportion of training and testing sets can influence the results of fault diagnosis.[29] Better diagnostic results will be acquired if the number of each fault type sample is more than 100 and the proportion of training sets exceeds 80 %. Thus, a total of 480 samples, with 120 samples for each fault type, were included in the dataset. Among them, 400 samples were randomly selected for training, while the remaining 80 samples were reserved for testing.

Firstly, several modal components can be acquired after processing by ACMD algorithm. Next, the feature vectors were constructed by calculating the permutation entropy of modal component. The final step was to use the constructed feature vectors and their corresponding labels as inputs to the CNN model for generator fault diagnosis The CNN model was trained for 500 iterations with a training batch size of 64 and a learning rate of 0.001. After completing the training, the confusion matrix of the invisible test set was demonstrated in Fig. 9, which shows that the model only misclassified a single sample, predicting a normal state as an eccentric fault. The accuracy curve of CNN model is represented in Fig. 10, where it can be observed that the accuracy of the model rapidly increases at the beginning of the iteration. Subsequently, the accuracy curve stabilizes at over 95 % after 50 iterations. After 200 iterations, the accuracy of fault classification approaches 100 % and keeps stable until the end of training. The y-axis at right side in Fig. 10 indicates the training loss of model. Training loss was a parameter used to calculate the difference between predicted value and true value. A smaller training loss indicates higher prediction accuracy of the model. After 350 iterations, the value of training loss decreases approximately to 0.02 and inclines to remains steady in subsequent iterations, indicating the model have achieved a convergence state.

To demonstrate the superiority of the proposed method, a comparison was made with other methods, including EEMD-PE-SVM, EEMD-PE-GA-BP, EEMD-PE-LSTM, EEMD-PE-CNN, VMD-PE-SVM, VMD-PE-GA-BP, VMD-PE-LSTM, VMD-PE-CNN, ACMD-PE-SVM, ACMD-PE-GA-BP, ACMD-PE-LSTM, and the results are presented in Fig. 11. As shown in Fig. 11, the 12 different diagnostic methods mentioned above are divided into four groups based on different classification algorithms. Through the comparison of the different groups, it can be found that an enormous gap exists between traditional machine learning classification algorithms and other deep learning networks. The first group using the SVM algorithm as a fault classifier obtains the worst results with only 80 % accuracy, while other neural network methods obtain superior results. Generator fault classification diagnosis is different from rotating machinery such as bearings and gears, which has a noticeable fault characteristic frequency. Not only the fault characteristic frequency of generator fault is not conspicuous, but also the difference between different faults is extremely small. For this reason, traditional machine learning algorithm is not applicable for generator fault classi-

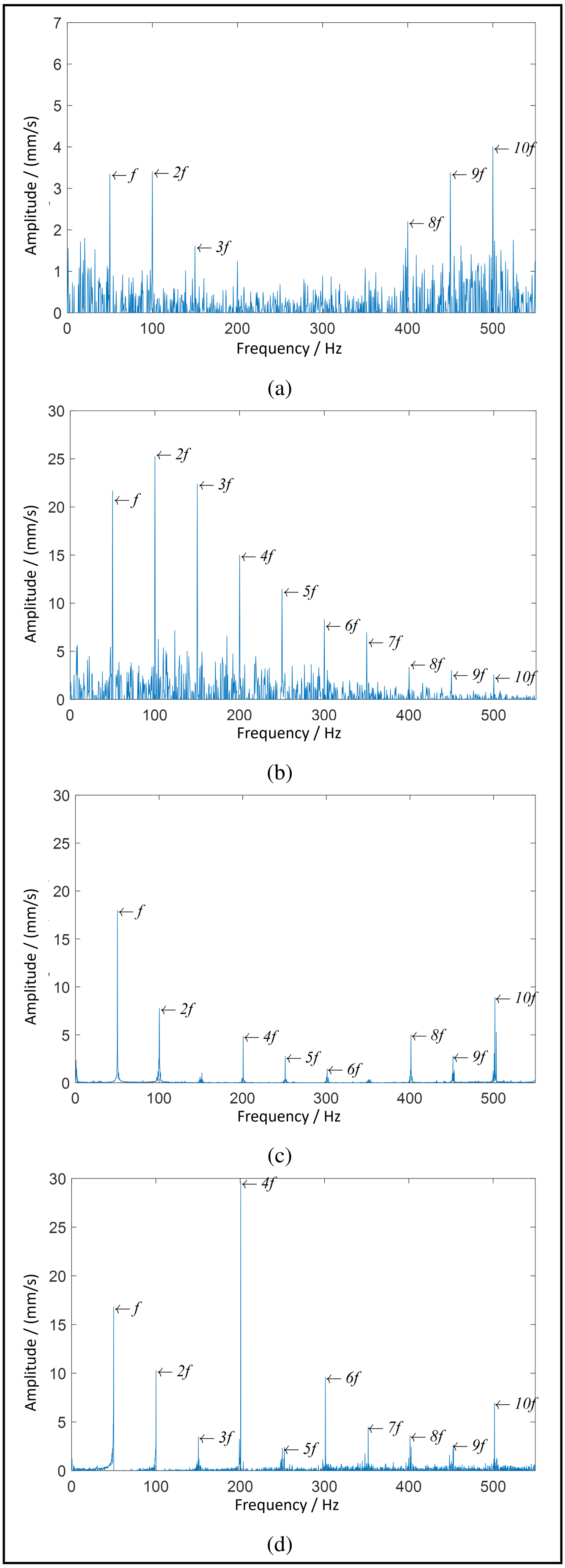

Figure 8. Envelope spectrum of simulation signal :(a) VMD envelope spectrum (b) ACMD envelope spectrum; Envelope spectrum of real signal :(c) VMD envelope spectrum (d) ACMD envelope spectrum..

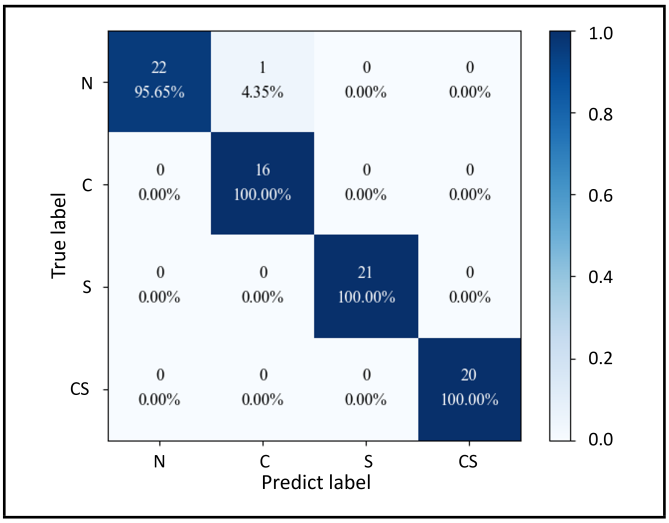

Figure 9. Confusion matrix representing the training results of CNN.

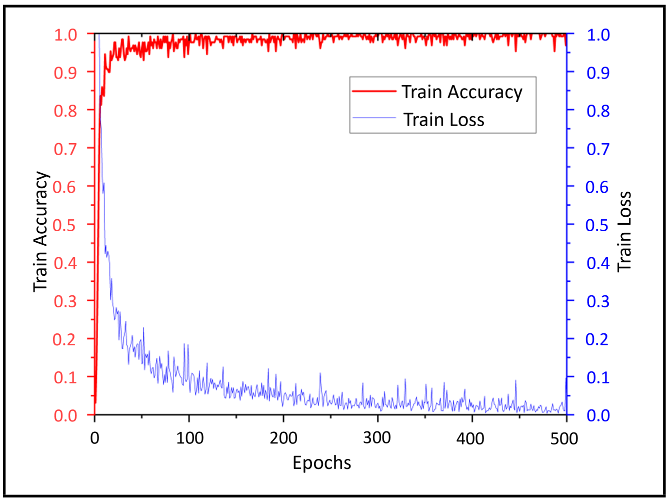

Figure 10. Fault diagnosis accuracy curve of ACMD-PE-CNN.

fication and diagnosis compared with the deep learning algorithms.

After observing Fig. 11, it can be found that the ACMD method can obtain superior results in fault classification compared with the EEMD and VMD methods when the fault classification algorithm is same, which reflects the superiority of ACMD in signal processing. The results obtained by the fourth group prove that the method using CNN algorithm as classifier can predict the type of fault with an accuracy of 98 %, which proves that CNN model has excellent superiority in fault classification. Overall, the results in Fig. 11 show that the diagnosis method of applying ACMD as decomposition algorithm and CNN network as classifier can realize the best diagnostic result. Then, the relationship between the accuracy curve of VMD-PE-LSTM, VMD-PE-CNN, ACMD-PE-LSTM, ACMD-PE-CNN, and the number of iterations is drawn in Fig. 12. As can be seen from Fig.12 that the diagnostic accuracy of CNN remained stable at over 90 % after 30-th iteration, while the accuracy of the LSTM network increased slowly, approaching high accuracy after 100th iteration. The result proves that CNN has superiority in terms of diagnostic accuracy and efficiency.

To present the feature information extracted from the model more intuitively, a method known as t-Distributed Stochastic

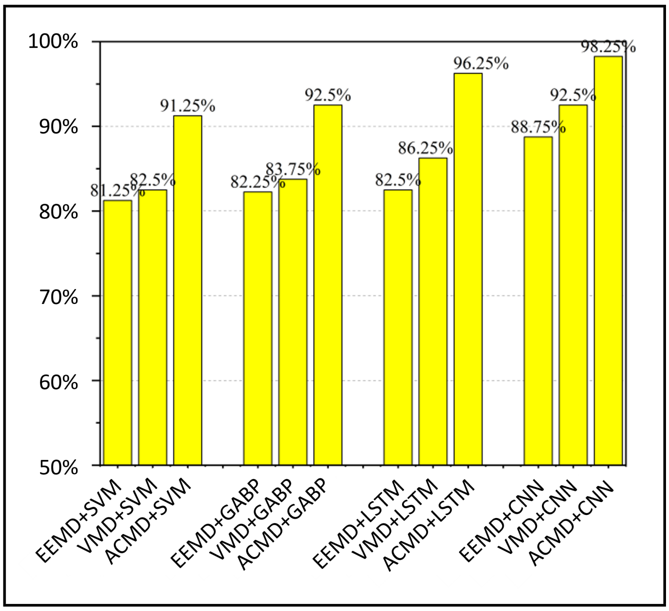

Figure 11. Comparison of different fault diagnosis methods.

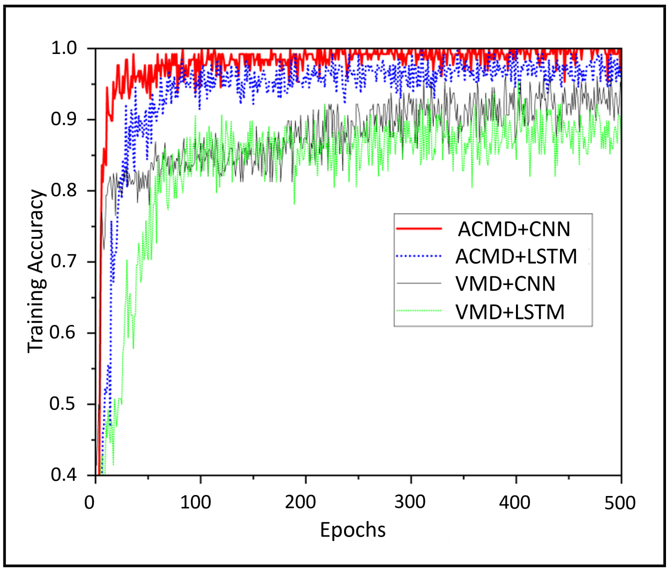

Figure 12. Accuracy curve for the neural network combination method using ACMD and VMD.

Neighbor Embedding (t-SNE) is applied to reduce the dimensionality in this paper. Through this method, the feature information of each sample extracted by the fault classification algorithm can be mapped into a visualized two-dimensional vector.

As visualized in Fig. 13, the fault feature information extracted from the hybrid model of ACMD+PE+CNN is transformed into a two-dimensional vector. It can be seen in Fig. 13, the model has learned the features that distinguish between different classes of generator situations, particularly normal state and the other three classes. Each of the four groups of feature vector vectors has a clear distinction from the other groups, with only one point that should have been in a normal state mistakenly classified as an eccentric fault. The result suggests that the model can correctly classify faults and achieve satisfactory results in practical applications.

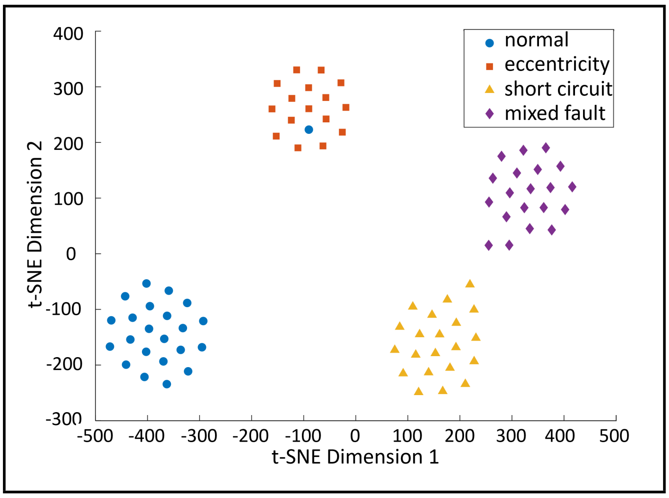

Figure 13. Visualization of the feature extracted from CNN, mapped into 2-dimensional vector.

5. CONCLUSIONS

Generators, as the most critical equipment in the power production system, are frequently suffering from different faults, resulting in serious human and material loss. To avoid this situation, this paper selects vibration signal to diagnose generator faults. However, the vibration signal of generator faults is weak in the early stage and is easily affected by environmental noise. At the same time, various mixed faults often occur simultaneously, making it difficult to diagnose manually through the spectrum feature obtained by traditional signal processing methods. Therefore, to complete the diagnosis of generator faults timely and accurately, this paper proposes a practical fault diagnosis method for generator using ACMD permutation entropy and the CNN network, combing advanced signal processing technology with the powerful classification function of neural networks to diagnose motor faults. Firstly, the original vibration signals are decomposed into several intrinsic mode functions by ACMD algorithm. Then the permutation entropy values of each component are calculated and construct the feature vectors, which are regarded as the input of CNN. Finally, CNN is utilized to classify the feature vectors obtained in the previous step to achieve the diagnosis of generator faults and obtains a classification accuracy of nearly 100 %. Below are the main conclusions drawn from the study:

1. The signal decomposition algorithm ACMD is employed for decomposing the generator vibration signal, which is found to be superior compared to other methods.

2. An entropy method called PE is applied to characteristic the fault feature of different types of generator fault.

3. The result of fault diagnosis based on CNN proves that it has excellent advantages over other classification models.

4. The proposed hybrid method achieves generator fault classification with the diagnostic accuracy of 98 %, which is higher than the comparison methods mentioned in this paper.

The experimental results indicate that the method proposed in this paper accurately diagnoses faults under actual engineering conditions and is of great significance for preventing various faults in generators and maintaining the stability and safety of the entire power system.

In future study, an improvement can be the inclusion of an appropriate optimization algorithm in the parameter selection process. Additionally, using multi-dimensional and multi-scale feature vectors as input for fault pattern recognition, and utilizing fault data under variable speed situations could also be considered in future research. Another potential research direction is investigating fault diagnosis under unbalanced data or small sample data, which has recently gained attention from many scholars.

ACKNOWLEDGEMENTS

This work is supported by National Natural Science Foundation of China (52177042), National Natural Science Foundation of Hebei Province (E2020502032), the Chinese Fundamental Research Funds for the Central Universities (2020MS114), the Top Youth Talent Support Program of Hebei Province ([2018]-27), and Suzhou Social Developing Innovation Project of Science and Technology (SS202134).

REFERENCES

[1] Y. L. He, *Analysis on mechanical and electrical characteristics of generator under air gap eccentricity and winding short circuit composite faults*, North China Electric Power University, (2012).

[2] T. Goktas, M. Zafarani, B. Akin, Discernment of broken magnet and static eccentricity faults in permanent magnet synchronous motors, *IEEE Transactions on Energy Conversion*, **31**(2), 578-587, (2016).

[3] I. O. Zaparoli, L. R. Baccarini, et al. Transient envelope current analysis for inter-turn short-circuit detection in induction motor stator, *Journal of the Brazilian Society of Mechanical Sciences and Engineering*, **42**(97), (2020). https://doi.org/10.1007/s40430-020-2188-7

[4] H. Z. Ma, et al. New fault diagnosis method for stator winding inter turn short circuit in synchronous condensers, *Electric Machines and Control*, **25**(9), 35-45, (2021).

[5] T. Y. Wang, Q. K. Han, F. L. Chu, Z. P. Feng, Vibration based condition monitoring and fault diagnosis of wind turbine planetary gearbox: A review, *Mechanical Systems and Signal Processing*, **126**, 662-685, (2019). https://doi.org/10.1016/j.ymssp.2019.02.051

[6] G. L. He, J. L. Li, K. Ding, Z. G. Zhang, Feature extraction of gear and bearing compound faults based on vibration signal sparse decomposition, *Applied Acoustics*, **189**, 108604, (2022). https://doi.org/10.1016/j.apacoust.2021.108604

[7] Y. J. Sun, S. H. Li, X. H. Wang, Bearing fault diagnosis based on EMD and improved Chebyshev distance in SDP image, *Measurement*, **176**, 109-110, (2021). https://doi.org/10.1016/j.measurement.2021.109100

[8] N. E. Huang, Z. Shen, Log Steven R., et al., The empirical mode decomposition and the Hilbert spectrum for nonlinear and non-stationary time series analysis, *Proceedings of the Royal Society A*, **454**, 903-995, (1998). https://doi.org/10.1098/rspa.1998.0193

[9] Z. H. Wu, N. E. Huang, A study of the characteristics of white noise using the empirical mode decomposition method, *Proceedings:Mathematical, Physical and Engineering Sciences*, **460**(2046), 1597-1611, (2004). https://doi.org/10.1098/rspa.2003.1221

[10] Z. Zheng, W. L. Jiang, H. S. Hu, et al., Research on rolling bearings fault diagnosis method based on EEMD morphological spectrum and kernel fuzzy C-means clustering, *Journal of Vibration Engineering*, **28**(02), 324-330, (2015).

[11] W. Xue, X. Dai, J. Zhu, Y. Luo, and Y. Yang, A noise suppression method of ground penetrating radar based on EEMD and permutation entropy, *IEEE Geoscience and Remote Sensing Letters*, **16**(10), 1625–1629, (2019). https://doi.org/10.1109/LGRS.2019.2902123

[12] Torres M. E., Colominas M. A., Schlott-Hauer G., et al., A complete ensemble empirical mode decomposition with adaptive noise, 2011 IEEE International Conference on Acoustics Speech and Signal Processing (ICASSP 2011). 4144-4147, (2011). https://doi.org/10.1109/ICASSP.2011.5947265

[13] Konstantin D., Dominique Z., Variational Mode Decomposition, *IEEE Transactions on Signal Processing*, **62**(3), 531-544, (2014). https://doi.org/10.1109/TSP.2013.2288675

[14] J. L. Chen, J. Pan, Z. P. Li, Y. Y. Zi, X. F. Chen, Generator bearing fault diagnosis for wind turbine via empirical wavelet transform using measured vibration signals, *Renewable Energy*, **89**, 80-92, (2016). https://doi.org/10.1016/j.renene.2015.12.010

[15] Antonio C., J. F. Liu, H. M. Zhou, Adaptive local iterative filtering for signal decomposition and instantaneous frequency analysis, *Applied and Computational Harmonic Analysis*, **41**(2), 384-411, (2016). https://doi.org/10.1016/j.acha.2016.03.001

[16] X. Wang, G. Tang, X. Yan, Y. He, X. Zhang and C. Zhang, Fault Diagnosis of Wind Turbine Bearing Based on Optimized Adaptive Chirp Mode Decomposition, *IEEE Sensors*, **21**(12), 13649-13666, (2021). https://doi.org/10.1109/JSEN.2021.3071164

[17] S. Chen, Y. Yang, Z. Peng, et al., Detection of rub-impact fault for rotor-stator systems: A novel method based on adaptive chirp mode decomposition, *Journal of Sound and Vibration*, **440**, 83-99, (2019). https://doi.org/10.1016/j.jsv.2018.10.010

[18] C. Zhang, C. J. He, S. Li, et al., A Hybrid Method to Diagnose 3D Rotor Eccentricity Faults in Synchronous Generators Based on ALIF_PE and KFCM, *Mathematical Problems in Engineering*, **2021**, 5513881, 14 pages, (2021). https://doi.org/10.1155/2021/5513881

[19] Namigtle-Jiménez, R. F. Escobar-Jiménez, J. F. Gómez-Aguilar, C. D. García-Beltrán, A. C. Téllez-Anguiano, Online ANN-based fault diagnosis implementation using an FPGA: Application in the EFI system of a vehicle, *ISA Transactions*, **100**, 358-372, (2020). https://doi.org/10.1016/j.isatra.2019.11.003

[20] J. Liu, Y. F. Li, Enrico Zio, A SVM framework for fault detection of the braking system in a high speed train, *Mechanical Systems and Signal Processing*, **87**, Part A, 401-409, (2017). https://doi.org/10.1016/j.ymssp.2016.10.034

[21] Z. S. Yang, C. Z Kong, Y. H. Wang, X. Rong, L. P. Wei, Fault diagnosis of mine asynchronous motor based on MEEMD energy entropy and ANN, *Computers & Electrical Engineering*, **92**, 107070, (2021). https://doi.org/10.1016/j.compeleceng.2021.107070

[22] X. Tang, B. Hu, & H. Wen, Fault Diagnosis of Hydraulic Generator Bearing by VMD-Based Feature Extraction and Classification, *Iranian Journal of Science and Technology, Transactions of Electrical Engineering*, **45**(4), 1227–1237, (2021). https://doi.org/10.1007/s40998-021-00421-0

[23] Jalayer M., Orsenigo C., Vercellis C., Fault detection and diagnosis for rotating machinery: A model based on convolutional LSTM, Fast Fourier and continuous wavelet transforms, *Computers in Industry*, **125**, 103378, (2021). https://doi.org/10.1016/j.compind.2020.103378

[24] J. Deng, W. Zhang, X. Yang. Recognition and classification of incipient cable failures based on variational mode decomposition and a convolutional neural network[J], *Energies*, **12**(10), 2005, (2019). https://doi.org/10.3390/en12102005

[25] D. Q. He, C. Y. Liu, Z. Z. Jin, R. Ma, Y. J. Chen, S. Shan, Fault diagnosis of flywheel bearing based on parameter optimization variational mode decomposition energy entropy and deep learning, *Energy*, **239**, Part B, 122108, (2022). https://doi.org/10.1016/j.energy.2021.122108

[26] L. Xiang, P. H. Wang, X. Yang, A. J. Hu, H. Su, Fault detection of wind turbine based on SCADA data analysis using CNN and LSTM with attention mechanism, *Measurement*, **175**, 109094, (2021). https://doi.org/10.1016/j.measurement.2021.109094

[27] C. Bandt and B. Pompe, Permutation entropy: a natural complexity measure for time series, *Physical Review Letters*, **88**(17), 174102, (2002). https://doi.org/10.1103/PhysRevLett.88.174102

[28] H. Yang, D. Y. Liu, L. P. Peng, DTCWT multi-scale joint entropy and CNN planetary gear fault diagnosis method, *Mechanical Design and Manufacturing*, **382**(12), 127-130+136, (2022).

[29] Q. C. Zhou, H. H. Shen, J. Zhao, et al. Bearing fault diagnosis based on improved stacked recurrent neural network, *Journal of Tongji University (natural science edition)*, **47**(10), 1500-1507, (2019). https://doi.org/10.3390/app10186359